A variable step size improved multiband-structured subband adaptive filter algorithm with subband input selection

Chang Liu, Zhi Zhang

***Abstract*—**Subband adaptive filter algorithms are able to improve the convergence behavior by performing the pre-whitening procedure on the input signals. In this paper, we propose a new variable step size improved multiband-structured subband adaptive filter algorithm which dynamically selects subband filters (VSS-DS-IMASF) in order to reduce the computational complexity. The subbband selection scheme which is designed to select the meaningful subbands is based on comparing the steady state subband mean square error (SMSE) with the subband error power throughout the algorithm execution, checking whether the subband filters converge to the steady state. In addition, the step size is controlled by the estimated mean square deviation (MSD) in order to achieve better steady state performance. Simulation results show that the proposed algorithm has lower steady state MSD and less computational complexities compared with the existing subband algorithms.

***Keywords*—**Normalized subband adaptive filter, Improved multiband-structured adaptive subband filter, Variable step size (VSS), Dynamic selection

I. Introduction

Subband adaptive filtering has been received much attention in recent years, due to its capability of improved convergence performance for highly correlated input signals. For the conventional subband adaptive filters(SAFs), the adaptive subfilter coefficients are updated independently in each subband, and thus the convergence performance is degraded by the band-edge and aliasing effects [1]. To overcome this drawback, several subband structures have been presented [2-6]. Pradhan-Peddy subband model [2] is designed by use of the polyphase decomposition and noble identity. Furthermore, combining the characteristics of the affine projection (AP) algorithm [7] with Pradhan-Peddy subband model, a subband AP (SAP) algorithm has been reported in [3], which improves the convergence rate and reduce the computational complexity of the AP algorithm. Lee and Gan [4] presented a normalized subband adaptive filter (NSAF) algorithm which made use of all the subband signals, normalized by their respective subband input variance, to update the full-band adaptive filter coefficients. Recently, to get better convergence performance, an improved multiband struct -ured subband adaptive filter (IMASF) algorithm has been proposed [5-6]. It applies the most recent P input signal vectors (projection orders) to participate in the full-band filter updating. The IMSAF algorithm can be considered as a generalized form of normalized least mean square (NLMS), AP and NSAF algorithms. However, it encounters higher computational complexity with the increased projection orders and long unknown system.

For SAFs, the convergence rate, steady state performance and computational complexity have been intensively investigated for many years. It is known that the fixed step size in SAFs reflects a tradeoff between fast convergence rate and low steady state misadjustment. To address this problem, several variable step size (VSS) subband algorithms have been proposed such as set-member NSAF (SM-NSAF)[8], VSS matrix for NASF [9], VSS-NASF [10-11], etc. The computational complexity is another subject for SAFs, it is showed that the computational complexity of SAF is depends on the number of subband [13]. Although the VSS subband algorithms mentioned above achieve both better steady state performance and the faster convergence simultaneously, their computational complexity remains invariant throughout the convergence process. Especially, they suffer from huge complexity for some applications such as acoustic echo cancellation (AEC) involving extremely long unknown system. Abadi and Husϕy have presented the simplified selective partial-update subband adaptive filter (SSPU-SAF) algorithm [12] with a lower computational complexity compared with the NSAF algorithm. The dynamic selective NSAF (DS-NSAF) presented in [13] adopts the subband filters dynamically based on the maximum mean square deviation (MSD) decrease principle, which retains the convergence performance and reduce the computational complexity. Song's selective subband scheme [14] is derived from the larger ratio of the squared error to an input power for each subband. It has better convergence performance and lower complexity. Yang [15] makes an analyses on the computational complexity of the IMSAF algorithm and proposes several simplified computation approaches to reduce its complexity. These simplified variants for IMSAF acquire the decrease of the complexity.

This work was supported in part by the National Natural Science Foundation of China under Grant 61501119.

Chang Liu, Zhi Zhang are with School of Electronic Engineering, Dongguan University of Technology, No.1, DaXue Avenue, Songshan Lake district, Dongguan, 523808, People's Republic of China (chaneaaa@163.com, ellon_zhang@sina.com).

For the subband number N=1 in the IMSAF, it is reckoned as AP algorithm [5]. Thus, the steady state subband mean square error (SMSE) for the IMSAF algorithm can be given through the idea illustrated in [16]. In this paper, we present a new VSS-IMSAF algorithm which dynamically selects subband filters in order to reduce the computational complexity. The variable step size is obtained based on the method of delay coefficients [17-18]. In addition, the subband selective criterion is derived by use of comparing the subband error power with the steady state SMSE. In other words, when a suband filter reaches its steady state, its adaptation is broke off. Thus, we call this proposed VSS-IMSAF as subband dynamic selection VSS-IMSAF (VSS- DS-IMSAF). Simulation results show that the proposed algorithm provides a lower steady-state normalized MSD (NMSD) compared to the existing subband algorithms. In addition, it gains a lower computational complexity.

The paper is organized as follows. The IMSAF algorithm is reviewed in Section 2. In Section 3, we derive the VSS-DS-IMSAF algorithm and its computational complexity is analysed. Simulation results are illustrated in Section 4, and Section 5 gives the conclusions.

II. IMSAF ALGORITHM

A. Review Stage

Consider the desired response $d(n)$ that arises from the model

$$d(n) = \mathbf{w}_o^T \mathbf{u}(n) + v(n). \tag{1}$$

where n is the time index, superscript T denotes transposition. $\mathbf{w}_o = [w_{o,0}, w_{o,1}, \cdots, w_{o,M-1}]^T$ is the unknown system of length M, $\mathbf{u}(n) = [u(n), u(n-1), \cdots, u(n-M+1)]^T$ is the input signal vector and $v(n)$ is the background noise, assumed to be zero mean ,and independent of $u(n)$, its variance is σ_v^2.

The structure of the IMSAF algorithm is shown in Fig. 1. The input signal $u(n)$ and desired signal $d(n)$ are partitioned into N subband signals $u_i(n)$ and $d_i(n)$ via the analysis filters $H_i(z)$, $i = 0,1,\cdots N-1$. The subband signals, $d_i(n)$ and $u_i(n)$ are critically decimated to a lower sampling rate commensurate with their bandwidth. We use the variable n to index the original sequences, and k to index the decimated sequence for all signals. The decimated subband signals can be defined as $y_{i,D}(k) = y_i(kN) = \mathbf{w}^T(k)\mathbf{u}_i(k)$ and $d_{i,D}(k) = d(kN)$, where $\mathbf{u}_i(k) = [u_i(kN), u_i(kN-1), \cdots, u_i(kN-M+1)]^T$ is the input data vector for the *i*th subband and the vector $\mathbf{w}(k) = [w_0(k), w_1(k), \cdots, w_{M-1}(k)]^T$ represents the fullband weight vector of the adaptive filter.

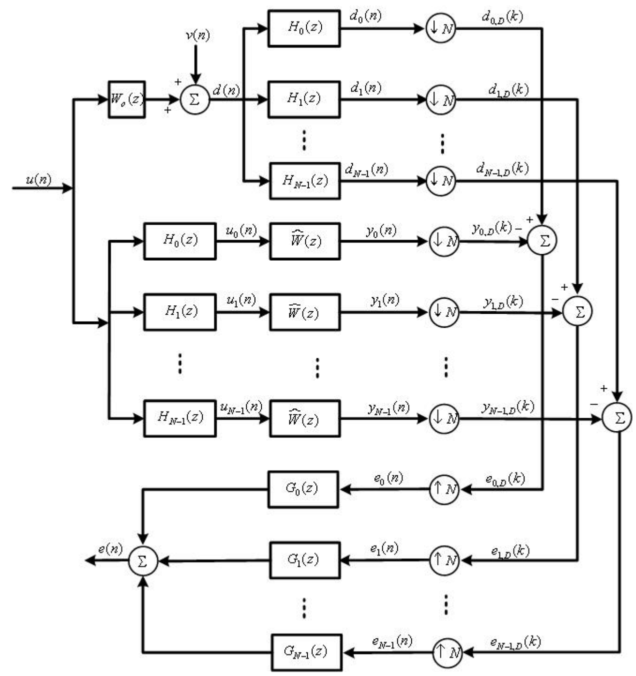

Fig. 1 Structure of the IMSAF

Define the input signal matrix $\mathbf{U}(k)$, the desired signal vector $\mathbf{d}_D(k)$, the estimated signal vector $\mathbf{y}_D(k)$, the subband noise vector $\mathbf{v}_D(k)$ and the error signal vector $\mathbf{e}_D(k)$ as follows

$$\mathbf{U}(k) = [\mathbf{U}_0(k), \quad \mathbf{U}_0(k), \quad \cdots, \quad \mathbf{U}_{N-1}(k)], \tag{2}$$

$$\mathbf{d}_D(k) = \left[\mathbf{d}_{0,D}^T(k), \quad \mathbf{d}_{1,D}^T(k), \quad \cdots, \quad \mathbf{d}_{N-1,D}^T(k)\right]^T, \tag{3}$$

$$\begin{aligned}\mathbf{y}_D(k) &= \left[\mathbf{y}_{0,D}^T(k), \quad \mathbf{y}_{1,D}^T(k), \quad \cdots, \quad \mathbf{y}_{N-1,D}^T(k)\right]^T \\ &= \mathbf{U}^T(k)\mathbf{w}(k),\end{aligned} \tag{4}$$

$$\mathbf{v}_D(k) = \left[\mathbf{v}_{0,D}^T(k), \quad \mathbf{v}_{1,D}^T(k), \quad \cdots, \quad \mathbf{v}_{N-1,D}^T(k)\right]^T, \tag{5}$$

$$\begin{aligned}\mathbf{e}_D(k) &= \left[\mathbf{e}_{0,D}^T(k), \quad \mathbf{e}_{1,D}^T(k), \quad \cdots, \quad \mathbf{e}_{N-1,D}^T(k)\right]^T \\ &= \mathbf{d}_D(k) - \mathbf{y}_D(k) = \mathbf{d}_D(k) - \mathbf{U}^T(k)\mathbf{w}(k).\end{aligned} \tag{6}$$

where

$$\mathbf{U}_i(k) = [\mathbf{u}_i(k), \quad \mathbf{u}_i(k-1), \quad \cdots, \quad \mathbf{u}_i(k-P+1)]^T, \tag{7}$$

$$\mathbf{d}_{i,D}(k) = \left[d_{i,D}(k), \quad d_{i,D}(k-1), \quad \cdots, \quad d_{i,D}(k-P+1)\right]^T, \tag{8}$$

$$\begin{aligned}\mathbf{y}_{i,D}(k) &= \left[y_{i,D}(k), \quad y_{i,D}(k-1), \quad \cdots, \quad y_{i,D}(k-P+1)\right]^T \\ &= \mathbf{U}_i^T(k)\mathbf{w}(k),\end{aligned} \tag{9}$$

$$\mathbf{v}_{i,D}(k) = \left[v_{i,D}(k), \quad v_{i,D}(k-1), \quad \cdots, \quad v_{i,D}(k-P+1)\right]^T, \tag{10}$$

$$\begin{aligned}\mathbf{e}_{i,D}(k) &= \left[e_{i,D}(k), \quad e_{i,D}(k-1), \quad \cdots, \quad e_{i,D}(k-P+1)\right]^T \\ &= \mathbf{d}_{i,D}(k) - \mathbf{y}_{i,D}(k) = \mathbf{d}_{i,D}(k) - \mathbf{U}_i^T(k)\mathbf{w}(k).\end{aligned} \tag{11}$$

By reusing the last P subband input vectors and solving the constrained optimization problem based on the principle of minimal disturbance, the updating equation of the IMSAF algorithm can be expressed as

$$\mathbf{w}(k+1) = \mathbf{w}(k) + \mu \mathbf{U}(k)[\mathbf{U}^T(k)\mathbf{U}(k) + \delta \mathbf{I}]^{-1}\mathbf{e}_D(k). \tag{12}$$

where μ is the step-size and δ is the regularization parameter which avoids division by zeros. $\mathbf{I}$ is a $NP \times NP$ identity matrix. Note that the weight vector is updated for each N input samples.

Because the cross-correlation of two arbitrary subband signals is small, the cross-correlation items in $\mathbf{U}^T(k)\mathbf{U}(k)$ can be neglected. Thus, a simplified version of the IMSAF algorithm (SIMSAF) is written as[15]

$$\mathbf{w}(k+1)=\mathbf{w}(k)+\mu\sum_{i=0}^{N-1}\mathbf{U}_i(k)\mathbf{R}_{i,i}^{-1}(k)\mathbf{e}_{i,D}(k). \tag{13}$$

where $\mathbf{R}_{i,i}(k)=\mathbf{U}_i^T(k)\mathbf{U}_i(k)+\delta\mathbf{I}_0$ is the subband autocorrelation matrix, and $\mathbf{I}_0$ is a $P\times P$ identity matrix.

Define the weight error vector $\Delta\mathbf{w}(k)=\mathbf{w}_o-\mathbf{w}(k)$, the undisturbed error vector $\boldsymbol{\xi}_D(k)$ can be given as $\boldsymbol{\xi}_D(k)=\mathbf{U}^T(k)\Delta\mathbf{w}(k)$, we get

$$\mathbf{e}_D(k)=\boldsymbol{\xi}_D(k)+\mathbf{v}_D(k). \tag{14}$$

Based on the maximum MSD decrease principle, the optimal step size of the IMSAF algorithm is expressed as [5]

$$\mu_{\text{opt}}(k)=\frac{E[\boldsymbol{\xi}_D^T(k)\mathbf{R}^{-1}(k)\mathbf{e}_D(k)]}{E[\mathbf{e}_D^T(k)\mathbf{R}^{-1}(k)\mathbf{e}_D(k)]}. \tag{15}$$

where $\mathbf{R}(k)=\mathbf{U}^T(k)\mathbf{U}(k)+\delta\mathbf{I}$, $E[\bullet]$ denotes the expectation operation . If the background noise is absent, we obtain $\mathbf{e}_D(k)=\boldsymbol{\xi}_D(k)$ from (14) and the fast convergence rate is achieved for $\mu_{\text{opt}}=1$.

III. Proposed IMSAF algorithm

A. Variable Step Size for IMSAF Algorithm

Assuming that the weight error vector $\Delta\mathbf{w}(k)$ is independent of the input $\mathbf{U}(k)$ [17], the undisturbed error power $\sigma_\xi^2(k)$ which is defined as $\sigma_\xi^2(k)=E[\boldsymbol{\xi}_D^T(k)\boldsymbol{\xi}_D(k)]$ can be approximated as [17-18]

$$\begin{aligned}\sigma_\xi^2(k)&=E[\boldsymbol{\xi}_D^T(k)\boldsymbol{\xi}_D(k)]\\&=E[\Delta\mathbf{w}^T(k)\mathbf{U}(k)\mathbf{U}^T(k)\Delta\mathbf{w}(k)]\\&=E\{tr[\Delta\mathbf{w}(k)\Delta\mathbf{w}^T(k)\mathbf{U}(k)\mathbf{U}^T(k)]\}\\&\approx(1/M)\,D(k)\cdot tr\{E[\tilde{\mathbf{R}}(k)]\}.\end{aligned} \tag{16}$$

where $D(k)=E[\|\Delta\mathbf{w}(k)\|^2]$ is defined as MSD, $\tilde{\mathbf{R}}(k)=\tilde{\mathbf{R}}^T(k)=\mathbf{U}^T(k)\mathbf{U}(k)$, $tr\{\bullet\}$ denotes the trace of a matrix and $\|\bullet\|^2$ represents Euclidean norm of a vector .

Neglecting the dependency of the input and noise, the numerator of (15) can be given by

$$\begin{aligned}&E[\boldsymbol{\xi}_D^T(k)\mathbf{R}^{-1}(k)\mathbf{e}_D(k)]\\&=E[\boldsymbol{\xi}_D^T(k)\mathbf{R}^{-1}(k)\boldsymbol{\xi}_D(k)]\\&=E\{tr[\boldsymbol{\xi}_D(k)\boldsymbol{\xi}_D^T(k)\mathbf{R}^{-1}(k)]\}\\&=E\{tr[\Delta\mathbf{w}^T(k)\mathbf{U}(k)\mathbf{U}^T(k)\Delta\mathbf{w}(k)\mathbf{R}^{-1}(k)]\}\\&\approx(1/M)\,D(k)\cdot tr\{E[\tilde{\mathbf{R}}(k)\mathbf{R}^{-1}(k)]\}.\end{aligned} \tag{17}$$

And then, the denominator of (15) can be written as

$$\begin{aligned}&E[\mathbf{e}_D^T(k)\mathbf{R}^{-1}(k)\mathbf{e}_D(k)]\\&=E[\boldsymbol{\xi}_D^T(k)\mathbf{R}^{-1}(k)\boldsymbol{\xi}_D(k)]+E[\mathbf{v}_D^T(k)\mathbf{R}^{-1}(k)\mathbf{v}_D(k)]\\&\approx(1/M)\,D(k)\cdot tr\{E[\tilde{\mathbf{R}}(k)\mathbf{R}^{-1}(k)]\}+\sigma_v^2 tr\{E[\mathbf{R}^{-1}(k)]\}.\end{aligned} \tag{18}$$

Using these results in (15)-(18), the optimal step size can be written as

$$\mu(k)=\frac{D(k)\cdot tr\{E[\tilde{\mathbf{R}}(k)\mathbf{R}^{-1}(k)]\}}{D(k)\cdot tr\{E[\tilde{\mathbf{R}}(k)\mathbf{R}^{-1}(k)]\}+M\sigma_v^2 tr\{E[\mathbf{R}^{-1}(k)]\}}. \tag{19}$$

Since the calculation of the expectation for input signal is not feasible in (19), we replace it by the instantaneous value. If the regularization parameter δ is very small enough and the input signals fluctuate slowly from one iteration to the next. (19) can be implemented as

$$\mu(k)=\frac{D(k)}{D(k)+\sigma_v^2 tr\{\mathbf{R}^{-1}(k)\}}. \tag{20}$$

For colored inputs, $\mathbf{R}(k)$ can only be approximated a block diagonal matrix[15]. However, for simplified calculation here, assuming that the diagonal components of $\mathbf{R}(k)$ is larger than the off-diagonal, we focus only on the diagonal components of $\mathbf{R}(k)$ [19], so the optimal step size can be approximated as

$$\mu(k)=\frac{D(k)}{D(k)+\sigma_v^2\sum_{i=0}^{N-1}\sum_{l=0}^{P-1}\left(1/\|\mathbf{u}_i(k-l)\|^2\right)}. \tag{21}$$

Note that the MSD cannot be calculated in practice due to the unknown system $\mathbf{w}_o$. We insert delay coefficients $\mathbf{h}(k)=[h_0(k), h_1(k),\cdots,h_{L-1}(k)]^T$ whose length is L prior to the adaptive filter artificially and the filter mismatch spreads evenly over all filter coefficients during the algorithm execution. Consequently, the MSD can be estimated as

$$\hat{D}(k)=\frac{M}{L}\|\mathbf{h}(k)\|^2. \tag{22}$$

B. Subband Steady State Mean Square Error

For analytical simplicity, we consider the simplified version of the IMSAF algorithm, then (13) can be expressed in terms of the weight error vector as

$$\Delta\mathbf{w}(k+1)=\Delta\mathbf{w}(k)-\mu\sum_{i=0}^{N-1}\mathbf{U}_i(k)\mathbf{R}_{i,i}^{-1}(k)\mathbf{e}_{i,D}(k). \tag{23}$$

Taking the expectation of the squared norm of the error weight vector in (23), we can obtain the MSD that satisfies

$$\begin{aligned}D(k+1)=D(k)&+\mu^2\sum_{i=0}^{N-1}E\{\mathbf{e}_{i,D}^T(k)\mathbf{R}_{i,i}^{-1}(k)\mathbf{e}_{i,D}(k)\}\\&-2\mu\sum_{i=0}^{N-1}E\{\boldsymbol{\xi}_{i,D}^T(k)\mathbf{R}_{i,i}^{-1}(k)\mathbf{e}_{i,D}(k)\}.\end{aligned} \tag{24}$$

When the algorithm reaches the steady state, the MSD satisfies $D(k+1)=D(k)$, as $k\to\infty$. Thus, from (24) we have

$$\mu^2\sum_{i=0}^{N-1}E\{\mathbf{e}_{i,D}^T(k)\mathbf{R}_{i,i}^{-1}(k)\mathbf{e}_{i,D}(k)\}=2\mu\sum_{i=0}^{N-1}E\{\boldsymbol{\xi}_{i,D}^T(k)\mathbf{R}_{i,i}^{-1}(k)\mathbf{e}_{i,D}(k)\}\quad \text{as } k\to\infty. \tag{25}$$

Assuming that the decimated subband signals are uncorrelated [20], the ith terms of summations on both side of (25) correspond to each other as follows

$$\mu^2E\{\mathbf{e}_{i,D}^T(k)\mathbf{R}_{i,i}^{-1}(k)\mathbf{e}_{i,D}(k)\}=2\mu E\{\boldsymbol{\xi}_{i,D}^T(k)\mathbf{R}_{i,i}^{-1}(k)\mathbf{e}_{i,D}(k)\}\quad i=0,1,\cdots,N-1,\ \text{as } k\to\infty. \tag{26}$$

Substituting (14) into (26), we obtain

$$(2-\mu)E\{\boldsymbol{\xi}_{i,D}^T(k)\mathbf{R}_{i,i}^{-1}(k)\boldsymbol{\xi}_{i,D}(k)\}=\mu E\{\mathbf{v}_{i,D}^T(k)\mathbf{R}_{i,i}^{-1}(k)\mathbf{v}_{i,D}(k)\}\quad i=0,1,\cdots,N-1,\ \text{as } k\to\infty. \tag{27}$$

Utilizing the assumption in [16] that $\mathbf{U}_i(k)$ is statistically independent of $\mathbf{e}_{i,D}(k)$ and $E\{\boldsymbol{\xi}_{i,D}^T(k)\boldsymbol{\xi}_{i,D}(k)\}=E\left|\xi_{i,D}(k)\right|^2\cdot S$ in the steady state, where $S \approx \mathbf{I}_0$ for small μ, and $S \approx (I \cdot I^T)$ for large μ, where $I^T = [1 \;\; 0 \;\; \cdots \;\; 0]$. Hence, the right-hand side (RHS) of (27) can be expressed as

$$\begin{aligned}&(2-\mu)E\{\boldsymbol{\xi}_{i,D}^T(k)\mathbf{R}_{i,i}^{-1}(k)\boldsymbol{\xi}_{i,D}(k)\}\\ &= (2-\mu)tr\{E[\boldsymbol{\xi}_{i,D}(k)\boldsymbol{\xi}_{i,D}^T(k)\mathbf{R}_{i,i}^{-1}(k)]\}\\ &= (2-\mu)E\left|\xi_{i,D}(k)\right|^2 tr\{S\cdot E[\mathbf{R}_{i,i}^{-1}(k)\}\\ &i = 0,1,\cdots,N-1, \text{ as } k\to\infty,\end{aligned} \tag{28}$$

and the left-hand side (LHS) of (27) can be given by

$$\mu E\{\mathbf{v}_{i,D}^T(k)\mathbf{R}_{i,i}^{-1}(k)\mathbf{v}_{i,D}(k)\} = \mu\sigma_{v_i,D}^2 tr\{E[\mathbf{R}_{i,i}^{-1}(k)]\} \quad i = 0,1,\cdots,N-1, \text{ as } k\to\infty, \tag{29}$$

where $\sigma_{v_i,D}^2$ is the subband noise and $\sigma_{v_i,D}^2 = \sigma_v^2/N$ [21].

Combining (27) , (28) with (29), we get the steady state subband excess mean square error (SEMSE) as

$$E\left|\xi_{i,D}(k)\right|^2 = \frac{\mu\sigma_{v_i,D}^2}{(2-\mu)}\frac{tr\{E[\mathbf{R}_{i,i}^{-1}(k)]\}}{tr\{S\cdot E[\mathbf{R}_{i,i}^{-1}(k)\}} \quad i = 0,1,\cdots,N-1, \text{ as } k\to\infty, \tag{30}$$

and therefore, the steady state subband MSE (SMSE) is given by

$$\text{SMSE} = \frac{\mu\sigma_{v_i,D}^2}{(2-\mu)}\frac{tr\{E[\mathbf{R}_{i,i}^{-1}(k)]\}}{tr\{S\cdot E[\mathbf{R}_{i,i}^{-1}(k)\}} + \sigma_{v_i,D}^2 \quad i = 0,1,\cdots,N-1, \text{ as } k\to\infty. \tag{31}$$

If the step size is small and $S \approx \mathbf{I}_0$, we have

$$\text{SMSE} = \frac{2\sigma_{v_i,D}^2}{2-\mu}, \tag{32}$$

and if $S \approx (I\cdot I^T)$, we get

$$\text{SMSE} = \frac{\mu\sigma_{v_i,D}^2}{2-\mu}tr\{\mathbf{R}_{i,i}(k)\}E[P/\|\mathbf{u}_i(k)\|^2] + \sigma_{v_i,D}^2. \tag{33}$$

C. Subband Selection Scheme

When a subband adaptive filter reaches the steady state, the error power for this subband approches the SMSE. Consequently, the continuous adaptation at this moment is un-meaningful and the reduction of error becomes not obvious. Along this line of thought, we select the meaningful subband inputs to update the filter weights based on checking whether the subband filters converge to the steady state. Therefore, by using of the SMSE presented in (32), the condition for subband input selection is

$$\|\bar{\mathbf{e}}_{i,D}(k)\|^2 > \frac{2P\sigma_{v_i,D}^2}{2-\mu} \to \|\bar{\mathbf{e}}_{i,D}(k)\| > \sqrt{\frac{2P}{2-\mu}}\sigma_{v_i,D}. \tag{34}$$

where $\|\bar{\mathbf{e}}_{i,D}(k)\|^2$ is defined the estimation for the ith subband error power, which can be computed as

$$\|\bar{\mathbf{e}}_{i,D}(k)\|^2 = \alpha\|\bar{\mathbf{e}}_{i,D}(k\text{-}1)\|^2 + (1-\alpha)\|\mathbf{e}_{i,D}(k)\|^2, \tag{35}$$

in addition , for simplified calculation here, we use (32) as SMSE for the suband selection.

Let $\Theta_{N(k)} = \{t_1, t_2, \cdots, t_{N(k)}\}$ denote a subset with $N(k)$ numbers of the set $\{0,1,\cdots,N-1\}$, where t_l means the index of the selected subband filters, and $N(k)$ is defined as the number of the selected subband filters at iteration k. Then, Substituting (21) into (13), and utilizing the subband selection scheme, the DS-VSS-MSAF algorithm is established as

$$\mathbf{w}(k+1) = \begin{cases}\mathbf{w}(k), & \text{if } N(k) = 0\\ \mathbf{w}(k+1) = \mathbf{w}(k) + \\ \mu(k)\sum_{l=0}^{N(k)}\mathbf{U}_{t_l}(k)\mathbf{R}_{t_l,t_l}^{-1}(k)\mathbf{e}_{t_l,D}(k), & \text{otherwise}\end{cases} \tag{36}$$

where $\|\mathbf{e}_{t_l,D}(n)\| > \sqrt{2P/[2-\mu(k)]}\sigma_{v_{t_l},D}$ $(l = 1,2,\cdots,N(k))$.

D. Computational Complexity

In this section, the computational complexity of the IMSAF, SIMSAF and proposed DS-VSS-IMSAF algorithms are compared, estimated by the number of multiplication for one iteration. Note that the weights of the subband adaptive filter is updated every N samples. For all three algorithms, the subband input signal and desired signal partition needs $(N+1)K$ multiplications, where K is the length of the analysis and synthesis filters. For error signal synthesis, the algorithms need K multiplications. For error estimation, due to the increased L taps of the adaptive filter for variable step size estimation, the DS-VSS-IMSAF requires $P(M+L)$ multiplications compared to PM multiplications needed in the IMSAF or SIMSAF algorithm. Using the recursive approach, calculation of auto-correlation matrix $\mathbf{U}^T(k)\mathbf{U}(k)$ requires $2PN^2$ multiplications for IMSAF, while the SIMSAF and DS-VSS-IMSAF need $2P$ and $2r(k)P$ multiplications for calculating subband auto-correlation matrix $\mathbf{U}_i^T(k)\mathbf{U}_i(k)$ respectively, where $r(k) = N(k)/N$ ($r(k) < 1$). It is well known that the $O\times O$ matrix inversion which can be performed with standard LU decomposition needs $O^3/2$ multiplications [22], where O is the rank of a square matrix. Consequently, for tap-weight adaptation, the MSAF needs $N^2P^3/2 + PM$ multiplications [15], the SIMSAF requires $P^3/2 + PM$ multiplications and the DS-VSS-IMSAF requires $r(k)[P^3/2 + P(M+L)]$ multiplications.

Table 1. Comparison of the computational complexities

Algorithm	Multiplications	Simulated Multiplications (in steady state) $K=128$ $M=1024$, $N=8$ $P=8$ $L=120$	Simulated Multiplication (in steady state) $K=128$ $M=1024$, $N=8$ $P=8$ $L=1200$
IMSAF	$N^2P^3/2+2PM$ $+2PN^2+(N+2)K$	35072	35072
SIMSAF	$P^3/2+2PM$ $+2P+(N+2)K$	17936	17936
DS-VSS-IMSAF	$r(k)[P^3/2+P(M+L)+2P]$ $+P(M+L)+(N+2)K+L+1$	12959	23915

In addition, the calculation of variable step size for the DS-VSS-IMSAF requires extra $L+1$ multiplications. For the DS-VSS-SAP, due to the small number of selected subband filters, the number of multiplication is reduced compared with the SIMSAF. On the other hand, the larger value of L results in the increasing multiplications, as can be seen in Table I. The simulated average multiplications per iteration is obtained by averaging over the 500 steady-state samples from 100 trials with AR(1) inputs illustrated in Section 4, μ=1.0 for the IMSAF and SIMSAF and μ(0)=1.0 for the DS-VSS-IMSAF. Hence, the proposed DS-VSS-IMSAF has lower overall computational complexity compared to the SIMSAF if the following inequality holds

$$L < \frac{[1-r(k)](P^3/2+PM+2K)-1}{r(k)+P+1}. \quad (37)$$

IV. Simulation results

To confirm the performance of the proposed algorithm in this paper, we present the simulation results of the proposed algorithm for the system identification and echo cancellation. All the following results are obtained by averaging over 100 Monte Carlo trials. An independent white Gaussian noise signal, $v(n)$,is added to the output of the unknown system, with 30-dB signal to noise ratio (SNR). Assume that the variance of noise is known, because it is can be easily estimated during silences and on line [23]. For signal partitioning in all experiments, The cosine-modulated filter banks [24] with subband number $N=8$ are used and the length of their prototype filter, K , is set to 128. The number of projection order $P=8$. The default values $\varepsilon=1\times10^{-4}$, $\alpha=0.9$ are employed. For the proposed algorithm, we choose the length of extended filter $L=120$. The performance is measured by use of normalized MSD (NMSD) defined as

$$\mathrm{NMSD}(k)=10\log_{10}\left(\frac{\|\mathbf{w}_o-\mathbf{w}(k)\|^2}{\|\mathbf{w}_o\|^2}\right). \quad (38)$$

In the first set of simulations, we evaluate the dynamic selection (DS) scheme for the IMSAF algorithm under the system identification. The IMSAF with DS-IMSAF algorithm are compared. The input is an AR(1) process with the coefficients (1,-0.9). The unknown system model is generated with coefficients being a white Gaussian noise sequence with zero-mean and unit variance, and its length is $M=1024$. For two algorithms, μ is set to 0.2 and 1, respectively. It can be seen from Fig. 2 that dynamic selection scheme leads to lower steady state NMSD with reduced computation complexity, while the convergence rate is decreased slightly due to the absent subband inputs, especially for large step size. Fig. 3 shows the average number of selected subbands of the DS-IMSAF, we can find that the number of selected subbands becomes small during the convergence phase. As a result, the DS scheme leads to low computational complexity for the tap-weight adaptation because of a fewer selected subbands.

The performances of the IMSAF, APA, NSAF, DS-NSAF, proposed VSS-IMSAF and VSS-DS-IMSAF algorithms are compared in Fig.4. Except for the VSS-IMSAF and VSS-DS-IMSAF algorithm, the step size μ is set to 0.6, and the initial step size $\mu(0)$ for two abovementioned VSS algorithms are set to 0.15. Other experimental parameters are identical with those in Fig.2. As shown in Fig.4, the proposed VSS-IMSAF and VSS-DS-IMSAF algorithms achieve the lowest steady state NMSD among these algorithms. However, due to the effect of the subband input selection, the convergence rate of the VSS-DS-IMSAF is lower than that of the IMSAF and VSS-IMSAF algorithms. Fig.5 shows the step size learning curve of the VSS-IMSAF, it is clear that the step size becomes small gradually, resulting in the lower NMSD, which ascribes to the step size controlled by MSD. In other words, the MSD decreases during the convergence process, so the variable step size which is presented in (21) inherits this property.

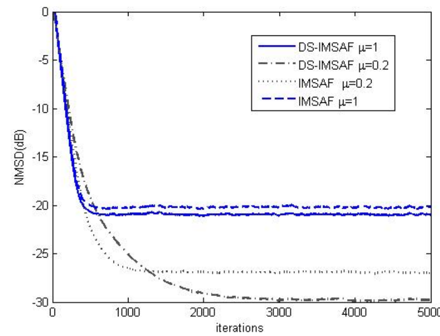

Fig. 2 NMSD curves of the IMSAF and DS-IMSAF.

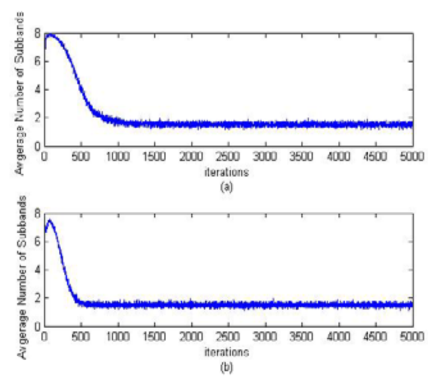

Fig. 3 Average number of selected subband (a) with $\mu=0.2$ (b) with $\mu=1$.

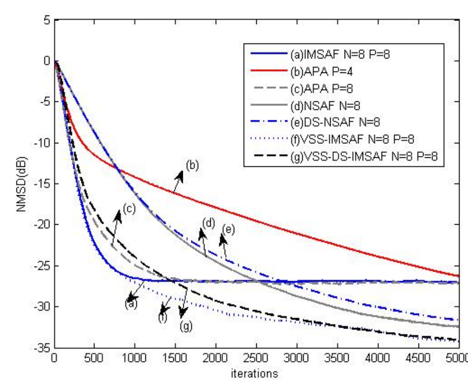

Fig. 4 NMSD curves of the IMSAF, APA, NSAF, DS-NSAF, proposed VSS-IMSAF and VSS-DS-IMSAF.

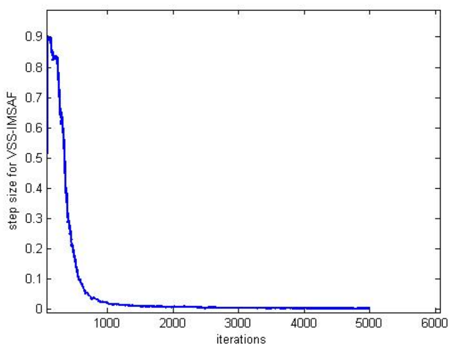

Fig. 5 Step size curve for the VSS-IMSAF.

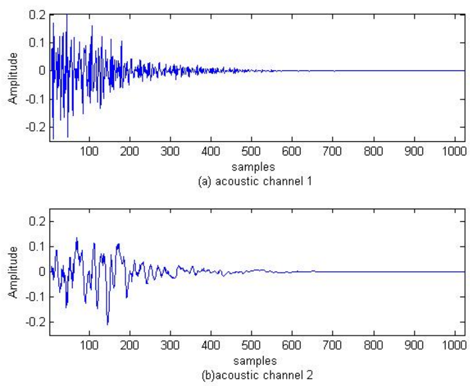

Fig. 6 Measured room acoustic impulse response.

Tracking ability is a very important issue for adaptive algorithms. In the second set of simulations, we focus on the tracking performance of these algorithms. The unknown systems to be identified is the acoustic echo responses of a room which are truncated to 1024 taps with a 8-kHZ sampling rate, as shown in Fig.6. In the experiments, the system sudden change occurs after 5000 iterations, from acoustic channel 1 show in Fig.6 (a) to acoustic channel 2 presented in Fig.6 (b). The input signal is generated by an AR(10) process with the coefficients (5.3217, -9.2948, 7.0933, -2.8125, 2.5805, -2.4230, 0.3747, 2.2628, -0.3028, 1.7444, 1.1053), which is highly colored signal like speech. Fig.7 shows that all three algorithms have good tracking performance after the sudden change of the unknown system. We also find that the VSS-IMSAF and VSS-DS- IMSAF can retain lower steady state NMSD. Fig.8 and Fig.9 show the tracking ability of the variable step size and average selected subband for the VSS algorithms. It can be seen that both step size and average selected subband are able to resist the occurrence of the sudden change for the unknown target system.

In the third set of simulations, we evaluate the performance of the proposed algorithms in the context of acoustic echo cancellation (AEC). Two acoustic channels shown in Fig.6 are also utilized. The speech signal input shown in Fig.10 (a) is sampled at 8kHz. Fig.10 (b) shows the near-end speech also sampled at 8kHz, which indicates the occurrence of the double

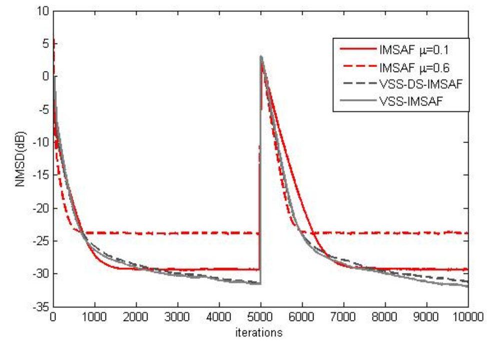

Fig. 7 NMSD curves of the IMSAF, VSS-IMSAF and VSS-DS-IMSAF for system sudden change

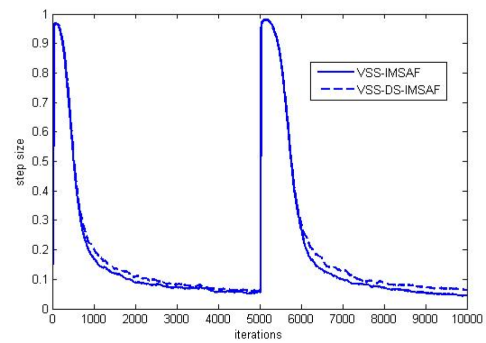

Fig. 8 Step size curves of the VSS-IMSAF and VSS-DS-IMSAF for system sudden change

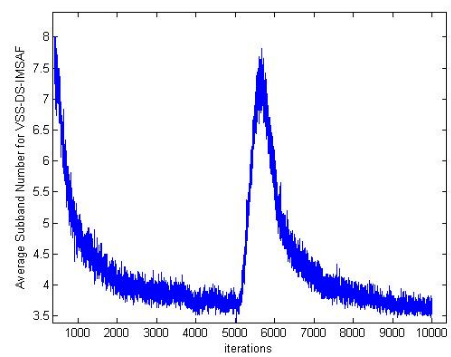

Fig. 9 Average number of selected subband of the VSS-DS-IMSAF for system sudden change.

-talk after 12.5s. Fig. 11 compares the NMSD curves of the IMSAF, VSS-IMSAF and VSS-DS-IMSAF algorithms. In this simulation, the system sudden change happens after 10s, from acoustic channel 1 to channel 2, and no near-end speech is present. It is can be seen that the two VSS algorithms have better steady state performance than the IMSAF algorithm. In Fig. 12, the algorithms are tested in the double-talk situation, the near-end speech presents after 12.5, which deteriorates the convergence performance for all three algorithms. However, we can see that two VSS algorithms also ensure more robust than the IMSAF algorithm.

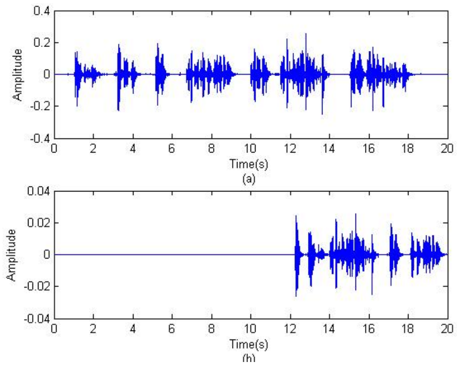

Fig.10. (a) Speech signal inputs. (b) Near-end speech occurred after 12.5s.

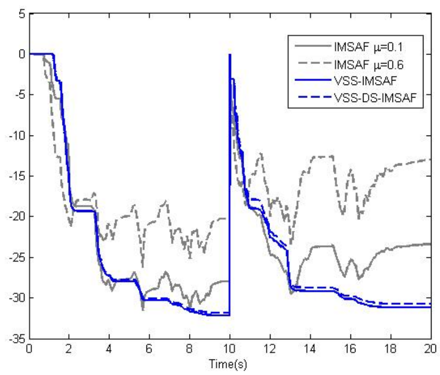

Fig.11 NMSD curves of the IMSAF, VSS-IMSAF and VSS-DS-IMSAF for system sudden change.

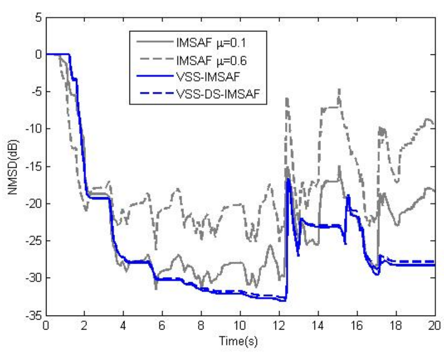

Fig.12 NMSD curves of the IMSAF, VSS-IMSAF and VSS-DS-IMSAF for double-talk situation.

V. Conclusion

In this paper, a new variable step size IMSAF algorithm with dynamic selection of subband filters is proposed. The variable step size is controlled by use of the MSD, which is estimated through the artificial delay coefficients. To design the subband input selection scheme, we check whether the subband filters converge to the steady state based on comparing the subband error power with the steady state subband MSE. The step size is optimized to maximize the MSD, and the meaningful subband inputs during the transient phase are selected. Simulation results, achieved in the context of the system identification and acoustic echo cancellation, demonstrate the proposed algorithm not only gains a lower NMSD compared with the existing SIMSAF algorithm, but also lessens the computational burden, only slightly encountering decrease of the convergence rate.

References

[1] K.A. Lee, W.S. Gan, and S.M. Kuo, *Subband Adaptive filtering: theory and implementation*. Chichester: Wiley, 2009, ch. 5.

[2] S. S. Pradhan, V. U. Reddy, "A new approach to subband adaptive filtering," *IEEE Trans. Signal Process.*, vol. 47, pp. 655–664, Mar. 1999.

[3] H. Choi, H. D.Bae, "Subband affine projection algorithm for acoustic echo cancellation," *EURASIP Journal on Advances in Signal Process.*, vol. 2006, pp. 1–12, Jan. 2007.

[4] K. A.Lee, W.S. Gan, "Improving convergence of the NLMS algorithm using constrained subband updates," *IEEE Signal Process. Lett.*, vol. 11, pp.736–739, Mar. 2004.

[5] F. Yang, M. Wu, P. Ji, and J. Yang, "An improved multiband-structured subband adaptive filter algorithm," *IEEE Signal Process. Lett.*, vol. 19, pp.647–650, July 2012.

[6] F. Yang, M. Wu, P. Ji, Z.Kuang, and J. Yang, "Transient and steady-state analyses of the improved multiband-structured subband adaptive filter algorithm," *IET Signal Process.*, vol. 9, pp.569–604, Oct. 2015.

[7] K.Ozeki, T. Umeda, "An adaptive filter algorithm using an orthogonal projection to an affine subspace and its properties," *Electron. Commun. Jpn.*, vol. 67-A, pp.19–27, May 1984.

[8] M. S. E.Abida, "Selective partial update and set-membership improved proportionate normalized subband adaptive filter algorithms," *International Journal of Adaptive Control & Signal Process.*, vol. 24, pp. 786–804, Sept. 2010.

[9] J. Ni, F. Li , "A variable step-size matrix normalized subband adaptive filter," *IEEE Trans. Audio, Speech, Lang. Process.*, vol. 18, pp. 1290–1299, Aug. 2010.

[10] J. W.Shin, N.W.Kong, and P. G.Park, "Normalized subband adaptive filter with variable step-size," *Electon. Lett.*, vol. 48, pp. 204–206, Feb. 2012.

[11] J. J. Jeong, K. Koo, G. T. Choi, and S. W. Kim, "A variable step-size for normalized subband adaptive filters," *IEEE Signal Process. Lett.*, vol. 19, pp.906–909, Oct. 2012.

[12] M. S. E.Abida, J. H. Husϕy, "Selective partial update and set-membership subband adaptive filters," *Signal Process.*, vol. 88, pp.2463–2471, Oct. 2008.

[13] S. E. Kim, Y. S.Choi, M. K.Song, and W. J. Song, "A subband adaptive filter algorithm employing dynamic selection of subband filters," *IEEE Signal Process. Lett.*, vol. 77, pp.245–248, Mar. 2010.

[14] M. K.Song, S. E. Kim, Y. S.Choi, and W. J. Song, "Selective normalized subband adaptive filter with subband extension," *IEEE Signal Process. Lett.*, vol. 60, pp.101–105, Mar. 2013.

[15] F. Yang, M. Wu, P. Ji, and J. Yang, "Low-complexity implementation of the improved multiband-structured subband adaptive filter algorithm," *IEEE Trans. Signal Process.*, vol. 63, pp.5133–5148, Oct. 2015.

[16] H.C.Shin, A.H. Sayed. "Mean-square performance of a family of affine projection algorithms," *IEEE Trans. Signal Process.*, vol. 52, pp.90–102, Jan. 2004.

[17] A. Mader, H. Puder, G. Schmit, H.C. Shin, A.H. Sayed. "Step-size control for echo cancellation filters-an overview," *Signal Process.*, vol. 80, pp.1697–1719, Sept. 2000.

[18] S. Haykin, *Adaptive Filter Theory*. Upper Saddle River, NJ: Prentice-Hall, 2002, ch. 3.

[19] S. J. Song, K. Y. Hwang, and W. J. Song, "An affine projection algorithm with dynamic selection of input vectors," *IEEE Signal Process. Lett.*, vol. 4, pp.529–532, Aug. 2007.

[20] K. A.Lee , W. S. Gan ,and S. M.Kuo, "mean-square performance analysis of the normalized subband adaptive filter," *in Proc. 40th Asilomar conf. Signals, Syst., Comput.*, Pacific Grove, CA, pp.248-252, 2006.

[21] W.Yin, A. Mehr, "Stochastic analysis of the normalized subband adaptive filter algorithm," *IEEE Trans. Circuits Syst. I: regular papers.*, vol. 58, pp.1020–1033, May 2011.

[22] B. Matin, " Multichannel affine and fast affine projection algorithms for active noise control and acoustic equalization systems," *IEEE Trans. Speech, Audio, Process.*, vol.11, pp.54–60, Jan. 2003.

[23] S. E.Kim, S. J.Kong, and W. J.Song, “An affine projection algorithm with evolving orders,” *IEEE Signal Process. Lett.*, vol. 16, pp.937–940, Nov. 2009.

[24] Y. P. Lin, P. P.Vaidyanathan, “A Kaiser window approach for the design of prototype filters of cosine modulated filter-banks,” *IEEE Signal Process. Lett.*, vol. 5, pp.132–134, June 1998.

Chang Liu received the B. S. degree in Electrical Engineering from the Hubei University of Technology, Wuhan, P. R. China, in 2005, the M. S. degree in Automation Engineering from the University of Electronic Science and Technology of China (UESTC) in 2008, and the Ph. D. degree in the School of Electronic Engineering, University of Electronic Science and Technology of China, Chengdu, P. R. China in 2012. His research interests include adaptive filter theory, adaptive equalization, synchronization， acoustic echo cancellation and feedback interference cancellation for on-channel repeaters.